Technobius, 2025, 5(2), 0079, DOI: https://doi.org/10.54355/tbus/5.2.2025.0079

Technobius
https://technobius.kz/

e-ISSN
2789-7338

Article

Studying the material orthotropy effect under the plane stress state of triangular plates

Moldir Beketova[1], Zhmagul Nuguzhinov[2], Serik Akhmediyev[1], Valentin Mikhailov[1], Omirkhan Khabidolda[3,*]

[1]A.S. Saginov Karaganda Technical University, Karaganda, Kazakhstan
[2]Kazakhstan Multidisciplinary Institute of Reconstruction and Development (KazMIRR), Karaganda, Kazakhstan
[3]E.A. Buketov Karaganda University, Karaganda, Kazakhstan
*Correspondence: oka-kargtu@mail.ru

Abstract. The article deals with the plane stress state of elastic thin orthotropic plates in the form of irregular triangles; orthotropy is assumed to be both physical and constructive. The research method used is the numerical finite difference method using a grid of scalene triangles. For such a grid, the authors have obtained resolving finite difference equations; in difference form they have obtained correct records of boundary conditions on the plate edges through the stress function based on the frame analogy taking into account the material orthotropy; typical finite difference equations are presented that allow solving problems of the plane stress state of triangular plates with a high degree of automation. As an illustrative example, a numerical calculation of triangular plates with a grid density of N = 8 is performed using a computer; the result of the study is the analysis of the stress state in the calculated grid nodes with a wide variation in the values of the a lateral edges angles of inclination to the base of the triangle, the orthotropy coefficients. The results obtained demonstrate the feasibility and effectiveness of using a finite difference scheme on irregular triangular grids for analyzing the plane stress state of orthotropic plates. The developed approach provides a solid theoretical foundation for modeling stress distributions in structures with geometric and material anisotropy. The flexibility of the method allows adapting it to a wide range of boundary conditions and geometric configurations, laying the groundwork for further analytical development and integration into engineering software tools for structural analysis.
Keywords: triangular plate, versatile grid, material orthotropy, frame analogy, finite-difference equations, stress state of plates, asymmetry of the geometric pattern, loading in the plane, stress orthotropy.

1. Introduction

The object of the study is plates of complex geometric outline in the form of an irregular triangle with different angles at their apexes. Such structural elements are widely used in construction, transport, mechanical engineering, power engineering, aircraft, and shipbuilding. Triangular plates in construction are used as connecting elements for utilities, as supports for lateral reinforcement, and also during the assembly and installation of shelving units. They are used to secure items such as air ducts and cable trays. Studying their stress-strain state (SSS) is a rather complex technical problem due to the difficulty of satisfying the boundary conditions in the presence of oblique edges; at the same time, the problem is complicated by the heterogeneity of the structure of the materials used, in particular by their orthotropy the difference in elastic properties in mutually perpendicular directions [1]. A lot of works deal with studying orthotropic plates. Among them, there are works [2], [3], [4].

In this regard, in the presence of many methods of studying the stress-strain state of objects of mechanics of a deformable solid in the form of two-dimensional structures (plates), it is advisable to use the numerical finite difference method (FDM); in this case, it is desirable to use a two-dimensional grid of scalene triangles that rationally approximates the surface of the plates in the form

of an irregular triangle. However, in this case, there is a problem of recording the boundary conditions on the oblique edges in finite differences; such a problem does not arise when calculating rectangular plates using a rectangular grid.

The paper [5] discusses the development of six low-order triangular finite elements intended for the linear static analysis of both thick-walled and thin-walled shell structures. The authors propose a combination of two plane-stressed triangular elements with three bending triangular elements, which allows the formation of three-node shell elements with 18 degrees of freedom. The paper [6] considers the complex behavior of an elastic triangular plate supported by a one-sided Winkler foundation, with an emphasis on studying forced vibrations. The work covers both static and dynamic analysis, including the cases of uniformly distributed load and eccentrically applied concentrated force. To construct the basic mathematical model, the authors use the Chebyshev series to approximate the displacement functions and the Lagrange method to obtain the equations of motion. Taking into account the nonlinear characteristics of the one-sided foundation, a numerical iterative solution method is developed that allows an adequate description of the interaction of the plate with the foundation. In the paper [7], a mixed finite element method is considered for modeling the bending of thin plates within the Kirchhoff–Love theory. The proposed approach is based on the use of triangular and parallelogram meshes and includes the construction of low-dimensional local functional spaces, as well as the corresponding degrees of freedom. These spaces provide consistency with a sufficiently rich tensor space and allow the implementation of all physically justified Dirichlet and Neumann boundary conditions. The paper [8] presents a generalized approach to modeling thin plates and shells based on six different models formulated using three types of curvature operators defined in the moving coordinate system. These models are designed to describe both residually flat and residually curved triangular meshes, which is especially important when modeling complex deformable surfaces. The paper [9] presents an analytical construction of the rigidity matrix of a structural element based on the Sierpinski triangle under transverse bending conditions. The approach does not rely on classical integration over volume or surface but is based solely on fundamental principles: symmetry, balance, and self-similarity inherent in fractal structures. Due to a high degree of symmetry and recursive structure of the Sierpinski triangle, it is shown that the resulting rigidity matrix can be expressed through a single material parameter that reflects the mechanical properties of the material. This allows for significant simplification of both the theoretical description and the numerical implementation of the model. The paper [10] presents the development and analysis of a new triangular element for modeling the bending of thin plates, taking into account the transverse shear effect. The DSPM3 element is based on the improvement of the existing T3γr element and has three degrees of freedom at each corner node, which makes it convenient for implementation in numerical methods.

Three-dimensional structures in the form of triangular plates of small and medium thickness with isotropic and orthotropic characteristics of materials were considered in the work [11]. The finite difference method was used with a grid of scalene triangles. Based on a numerical algorithm and proprietary programs, the parameters were calculated for transverse and planar loading for various boundary conditions.

In the study [12], the bending behavior of elastic isotropic plates shaped as arbitrary triangles is considered under various types of boundary conditions, such as hinged or clamped (rigidly fixed) edges. In this case, the finite element method (FEM) is employed. As an illustrative example, the study presents the bending of a right-angled triangular plate with hinged support along its perimeter. In studies [13], [14], a calculation method based on the shape factor with the use of affine transformations is proposed for calculating triangular plates. The bending stress-strain state of the plates is considered, including cases of free vibrations. In this case, the plate material can be isotropic or orthotropic. In work [15], the finite element method is used to study free vibrations of thin isotropic triangular plates in the presence of a hole, with the edges being hinged and clamped. A comparison of the obtained results with the data of the experimental method is carried out, and the error was up to 6%. In work [16] a thin triangular plate of arbitrary shape is considered; for free vibrations the numerical method is used under complex boundary conditions, including that in the presence of

supports inside the plate region. In work [17], the analysis of vibration processes and multi-criteria optimization of a rigid triangular plate were performed. Structurally, the triangular plate included stiffeners located relative to one of its sides. The resolving equation for the transverse bending of the plate was obtained taking into account the effect of the orthotropy parameters and external disturbance. The initial differential equation of the system was obtained based on the Bubnov-Galerkin method. Then, multi-objective optimization was carried out taking into account two objective functions: the nonlinearity of the system and the amplitude of oscillations. There were considered the following interrelated parameters: the plate thickness, its geometry, and the distance between the stiffeners. The effect of the initial parameters on the optimal solutions and their distribution were also studied.

The force vibration in the plane of an arbitrary layered triangular plate with complex boundary conditions was studied by the Chebyshev-Ritz method in work [15]. The coordinate transformation allowed reducing the triangular layered plate of arbitrary shape to an equivalent square plate. After the transformation, the displacement functions of the square plate were expressed through two-dimensional Chebyshev polynomials with the corresponding coefficients. Arbitrary elastic boundary conditions were modeled by adjusting the stiffness of each spring using the method of conditional virtual springs. The characteristics of free vibrations of a triangular layered plate under various boundary conditions were calculated. Reliability of the method was confirmed by comparison with the results obtained by the finite element method, as well as with experimental data. The analysis showed that the proposed method had high convergence and sufficient calculation accuracy.

The bending of cantilever triangular plates with the same angles of inclination of the lateral faces to the base was studied in work [18]. The finite difference method was used for the analysis. The results obtained were combined to solve the problem of the acute angle effect at the top of the plate. The calculations of a cantilever beam with variable bending rigidity were compared with similar calculations of a triangular plate reinforced along the contour using a reduction factor. The theoretical provisions and practical results of this study can be partially applied to study the bending of orthotropic scaled triangular plates with reinforcement along the edges.

The frequencies and modes of free vibrations of thin isotropic triangular plates with a central hole were studied under various boundary conditions in work [19]. The finite element method was used for the analysis. The spectrum of vibration modes of some triangular plates was compared with similar characteristics of square plates with hinged and rigid edge fixation. The presented numerical values of natural frequencies and vibration modes of triangular plates showed good agreement with the experimental data.

For the analytical solution to the problem of free vibrations of regular triangular plates, the simplified superposition method was used in work [20]. The problem was solved by dividing it into three subproblems, which were solved by symplectic methods by imposing a separation of variables on the control equation based on the Hamiltonian system and a symplectic expansion in eigenvalues. Then, analytical solutions were obtained for the frequency and mode shape, requiring equivalence between the original problem and the superposition. Comparison with numerical results for regular triangular plates confirmed the convergence and accuracy of the approach. Thus, the analysis of scientific research in the field of triangular plates shows that, despite the wide range of boundary conditions under consideration, many authors avoid their calculations due to the complexity of the fastening conditions. The proposed calculation method will allow solving the future problems of the plane stress state of triangular plates with complex loading patterns along their contour.

The main goal and objectives of the study are as follows. The authors of the article developed a specialized program for calculating the plane stress state (with the grid density of N=8) with a high degree of automation that ensured the calculation of all the types of stress in the median plane. The main goal is also developing a numerical finite difference method using a grid of scalene triangles, including implementation of boundary conditions and the development of an algorithm for solving problems of the plane stress state.

2. Methods

Let us consider the plane stress state of triangular orthotropic plates under their all-round compression by a uniformly distributed load of intensity “q” (Figure 1); in the general case, it is accepted that α≠β.

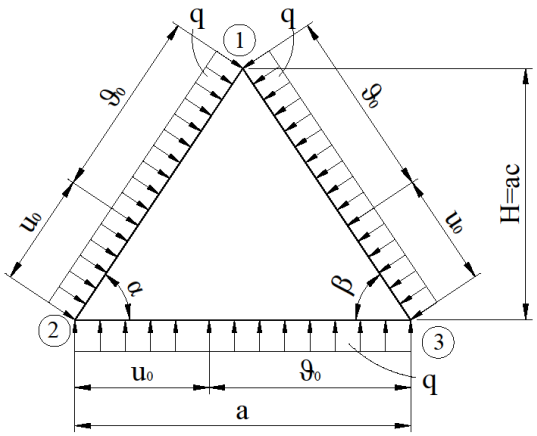

Figure 1 – Computational pattern of the plate

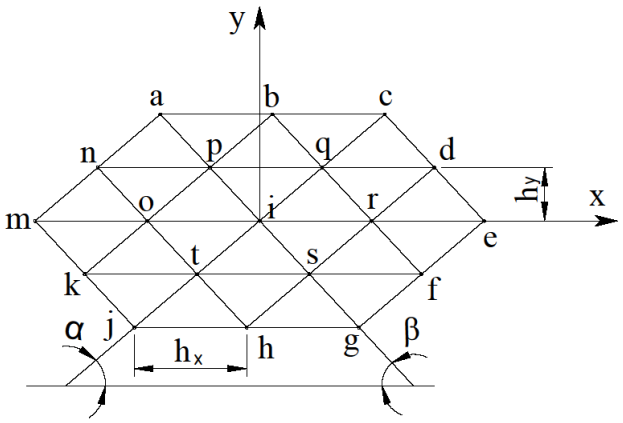

Figure 2 – Fragment of a grid of scalene triangles

The original fourth-order differential equation with variable coefficients has the form [21]:

$$\frac{\partial^4 F}{\partial x^4}+\alpha_0\frac{\partial^4 F}{\partial x^2\partial y^2}+\beta_0\frac{\partial^4 F}{\partial y^4}=0, \tag{1}$$

where F=F(x, y) is the stress function. The orthotropy coefficients:

$$\alpha_0=\frac{2a_{12}+a_{66}}{a_{22}}=E_2\left(\frac{1}{G}-\frac{2\nu_2}{E_1}\right),\ \ \beta_0=\frac{a_{11}}{a_{22}}=\frac{E_2}{E_1} \tag{2}$$

Stresses in the midplane of the plates are expressed through the stress function "F", which is as follows:

$$\sigma x=\frac{\partial^2 F}{\partial y^2};\quad \sigma y=\frac{\partial^2 F}{\partial x^2};\quad \tau_{xy}=-\frac{\partial^2 F}{\partial x\partial y}. \tag{3}$$

The finite difference operators for the *i*-th node of the triangular grid included in equation (1) were obtained earlier [1].

Then equations (1) for the *i*-th node (Figure 2) will take the following form (without taking into account the boundary conditions):

$$\begin{aligned}&\psi_1F_1+\psi_2(F_0+F_r)+\psi_3(F_p+F_s)+\psi_4(F_q+F_t)+\psi_5(F_n+F_f)+\psi_6(F_b+F_h)+\\&+\psi_7(F_d+F_k)+\psi_8(F_m+F_e)+\psi_9(F_a+F_g)+\psi_{10}(F_c+F_y)=0,\end{aligned} \tag{4}$$

where:

$$\begin{aligned}\psi_1&=6C^4+\alpha_0C^2(-6AB+4)+\beta_0\left[4(AB-1)^2+2(AB)^2+2A^2+2B^2\right],\\ \psi_2&=-4C^4+\alpha_0C^2(4AB-2)+\beta_0\left[-4AB(AB-1)+2AB\right],\\ \psi_3&=\alpha_0C^2(B-2A)+\beta_0\left[4A(AB-1)-2AB^2\right],\\ \psi_4&=\alpha_0C^2(A-2B)+\beta_0\left[4B(AB-1)-2A^2B\right],\\ \psi_5&=\alpha_0C^2A-2\beta_0A^2B;\ \ \psi_6=2\beta_0AB;\ \ \psi_7=\alpha_0C^2B-2\beta_0AB^2;\\ \psi_8&=C^4-\alpha_0C^2AB+\beta(AB)^2;\ \ \psi_9=\beta_0A^2;\ \ \psi_{10}=\beta_0B^2,\end{aligned} \tag{5}$$

here (the triangular grid parameters):

$$A=\frac{\sin\beta\cos\alpha}{\sin(\alpha+\beta)};\quad B=\frac{\sin\alpha\cos\beta}{\sin(\alpha+\beta)};\quad C=\frac{\sin\alpha\sin\beta}{\sin(\alpha+\beta)};$$

$$U=C^2-AB=-\frac{\sin\alpha\sin\beta\cos(\alpha+\beta)}{\sin^2(\alpha+\beta)};\quad h_x=a/N;\quad h_y=h_x a. \tag{6}$$

where: N is the number of divisions of the triangle sides ("grid density").

With (α_0=2; β_0=1), according to (4, 5) there is a special case of the plane stress state for isotropic triangular plates [1].

The boundary conditions along the edges of the plate (Figure 3) are also written in finite differences in the form of a frame analogy (taking into account the orthotropy of the material) [1], [21]:

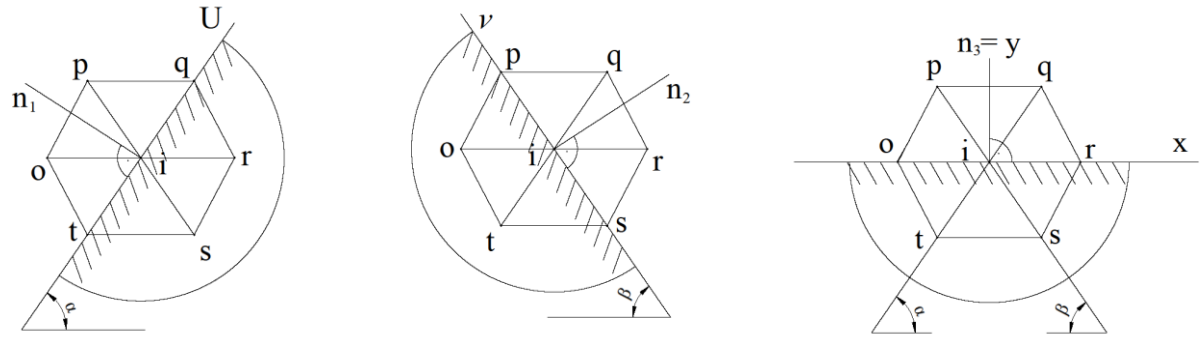

a) left edge b) right edge c) edge on the triangle base

Figure 3 – Towards the boundary conditions

$$F_i=\pm M_i;\quad \partial F_i/\partial nj=N_i\,(j=1,2,3), \tag{7}$$

where (M_i, N_i) are nodal values of the bending moment and longitudinal force in the main system that is a statically determinate and geometrically unchangeable frame, the rods of which are the edges (sides) of a given triangular plate.

Expressions (7) will take the following form at the nodes of the triangular grid:

a) along the left edge (Figure 3a) (j=1):

$$(0.5\psi_5^{*}F_0+\psi_9F_p)=\frac{\sin\alpha}{2h_y\cdot C}(0.5\psi_5F_r+\psi_9F_s)+\frac{2h_y\cdot C}{\sin\alpha}(N_i) \tag{8}$$

b) along the right edge (Figure 3b) (j=2):

$$(0.5\psi_7F_r+\psi_{10}F_q)=\frac{\sin\beta}{2h_y\cdot C}(0.5\psi_7F_0+\psi_{10}F_t)+\frac{2h_y\cdot C}{\sin\beta}(N_i); \tag{9}$$

c) along the triangle base (Figure 3c) (j=3):

$$(0.5\psi_6F_s+\psi_{10}F_t)=\frac{1}{2h_y}(0.5\psi_6+\psi_{10}F_q)+2h_y(N_i). \tag{10}$$

Based on the main finite-difference equation (4), taking into account expressions (8-10), excluding the stress functions of the contour and edge nodes of the triangular grid, typical finite-difference equations are obtained for triangular plates at arbitrary values of the "oblique" angles α and β (Figure 1); the number of which is equal to seven (Figure 4): I - for intra-contour nodes; II - for grid nodes near the left edge (1-2); III - the same, near the right edge (1-3), IV - the same, near the edge (2-3), at the base of the triangle; V - at the apex of the triangle (1); VI - the same, at the apex (2); VII - the same, at the apex (3). The entry of typical finite-difference equations is given in Table 1.

Table 1 – Standard finite-difference equations of the plane stress state of orthotropic triangular plates

No.	i	o	r	p	s	q	t	n	f	b	h	d	k	m	e	a	g	c	j	right part
I	Ψ_1	Ψ_2	Ψ_2	Ψ_3	Ψ_3	Ψ_4	Ψ_4	Ψ_5	Ψ_5	Ψ_6	Ψ_6	Ψ_7	Ψ_7	Ψ_8	Ψ_8	Ψ_9	Ψ_9	Ψ_{10}	Ψ_{10}	P_I
II	Ψ_1+(Ψ_8+Ψ_9)		Ψ_2		Ψ_3	Ψ_4+0.5 Ψ_5	Ψ_4+0.5 Ψ_5		Ψ_5		Ψ_6	Ψ_7			Ψ_8		Ψ_9	Ψ_{10}	Ψ_{10}	P_{II}
III	Ψ1+(Ψ8++Ψ10)	Ψ_2		Ψ_3+0.5Ψ	Ψ_3+0.5Ψ		Ψ_4	Ψ_5			Ψ_6		Ψ_7	Ψ_8		Ψ_9	Ψ_9		Ψ_{10}	P_{III}
IV	Ψ1+(Ψ8+ Ψ10)	Ψ_2+0.5Ψ_6	Ψ_2+0.5Ψ_6	Ψ_3		Ψ_4		Ψ_5		Ψ_6		Ψ_7		Ψ_8	Ψ_8	Ψ_9		Ψ_{10}		P_{IV}
V	Ψ1+(2Ψ8+Ψ9+ Ψ10)				Ψ_3+0.5Ψ		Ψ_4+0.5Ψ_5				Ψ_6					Ψ_9			Ψ_{10}	P_V
VI	Ψ_1+(2Ψ_9+ Ψ_8+Ψ_{10})		Ψ_2+0.5Ψ			Ψ_4+0.5Ψ						Ψ_7			Ψ_8			Ψ_{10}		P_{VI}
VII	Ψ_1+(2Ψ_{10}+Ψ_8+ Ψ_9)	Ψ_2+0.5Ψ_6		Ψ_3+0.5Ψ				Ψ_5						Ψ_8		Ψ_9				P_{VII}

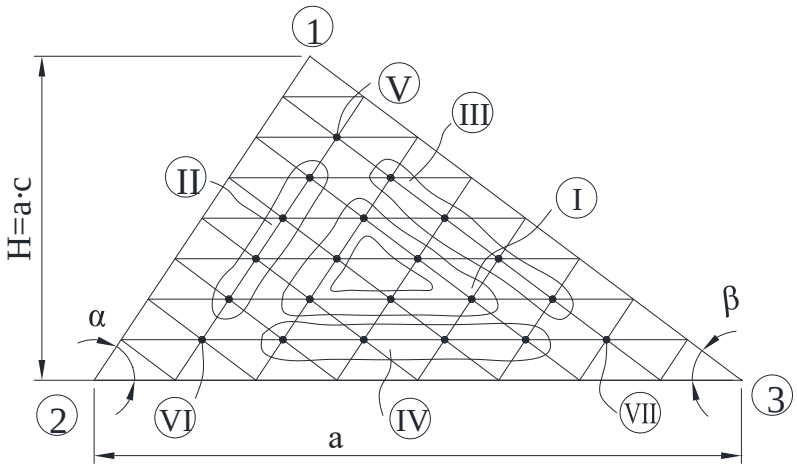

Figure 4 – Numbering of typical finite difference equations

The right parts of standard equations $P_i(i=1,2,...7)$ are written as follows (Table 1):

$$P_I = 0;\quad P_I = 0; P_{II} = -(\psi_2 M_o + \psi_3 M_p + \psi_6 M_b + \psi_7 M_k) - \frac{2h_y C}{\sin\alpha}(N_0 + N_p);$$

$$P_{III} = -(\psi_2 M_r + \psi_4 M_q + \psi_6 M_b + \psi_5 M_f) - \frac{2h_y C}{\sin\beta}(N_r + N_q);$$

$$P_{IV} = -(\psi_3 M_s + \psi_4 M_t + \psi_5 M_f + \psi_7 M_k) - 2h_y(N_t + N_s);$$

$$P_V = -(\psi_2 M_o + \psi_2 M_r + \psi_3 M_p + \psi_4 M_q + \psi_6 M_b + \psi_5 M_f + \psi_7 M_k) -$$

$$-2h_y C\left[\frac{1}{\sin\alpha}(N_0 + N_p) + \frac{1}{\sin\beta}(N_r + N_q)\right]; \qquad (11)$$

$$P_{VI} = -(\psi_2 M_0 + \psi_3 M_p + \psi_7 M_k + \psi_4 M_t + \psi_3 M_s + \psi_5 M_f + \psi_6 M_b) -$$

$$-2h_y C\left[\frac{1}{\sin\alpha}(N_0 + N_p) + (N_s + N_t)\right];$$

$$P_{VII} = -(\psi_2 M_s + \psi_4 M_q + \psi_4 M_t + \psi_6 M_b + \psi_2 M_r + \psi_5 M_f + \psi_7 M_k) -$$

$$-2h_y C\left[\frac{1}{\sin\beta}(M_r + N_q) + (N_s + N_t)\right].$$

Here (M_i, N_i) are nodal values of the bending moment and longitudinal force in a three-hinged contour frame (1-2-3) from a given compressive load “q” acting on the edges of the triangular plate (Figure 1).

To compare the obtained results, a study of the plane stress state for a triangular plate was conducted using the ANSYS program. The following parameters for orthotropic material were selected (Figure 5) and scheme of apply loads (Figure 6):

Properties of Outline Row 4: ortho

	A	B	
1	Property	Value	
2	Material Field Variables	Table	
3	Orthotropic Elasticity		
4	Young's Modulus X direction	1,5E+11	Pa
5	Young's Modulus Y direction	3E+11	Pa
6	Young's Modulus Z direction	1E+11	Pa
7	Poisson's Ratio XY	0,1	
8	Poisson's Ratio YZ	0,2	
9	Poisson's Ratio XZ	0,1	
10	Shear Modulus XY	1,42E+10	Pa
11	Shear Modulus YZ	1E+10	Pa
12	Shear Modulus XZ	1E+10	Pa

Figure 5 – Orthotropic material properties

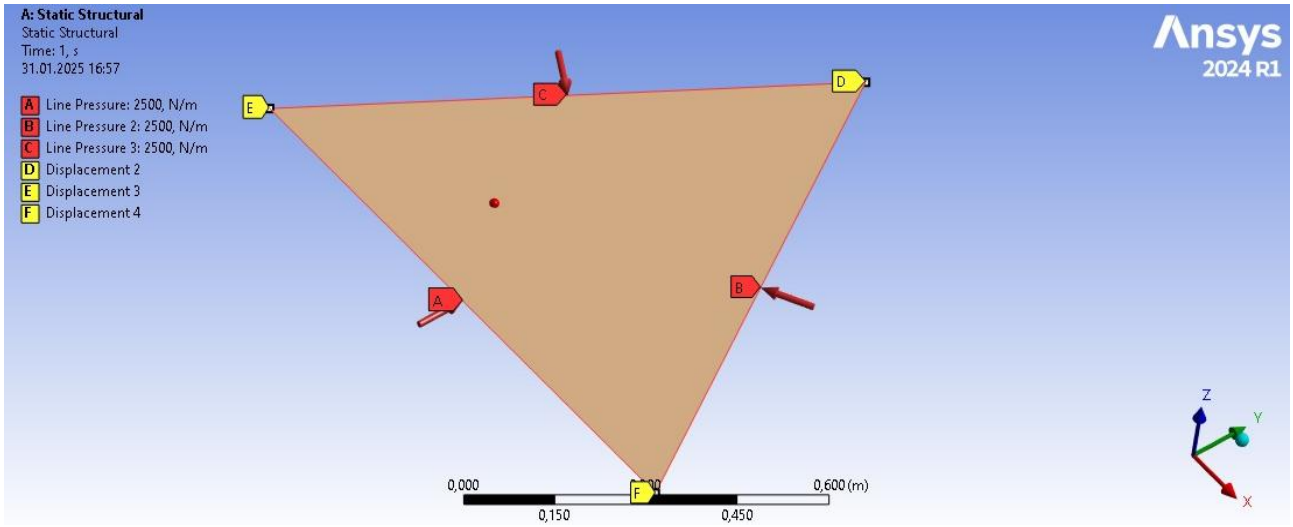

Figure 6 – Load parameters

3. Results and Discussion

The calculation algorithm when using the finite difference method for calculating the plane stress state of triangular plates is as follows [1], [4]. The surface of the plate is covered with a triangular grid with the number of divisions of its sides into "N" equal parts; Figure 7 shows the numbering of the calculated nodes of the grid from scalene triangles with the number of divisions of the sides N=8; here: (1, 2, …, 21) is the numbering of the intra-contour grid nodes; (I, II, …, XII) is the numbering of the grid nodes on the edges of the triangular plate.

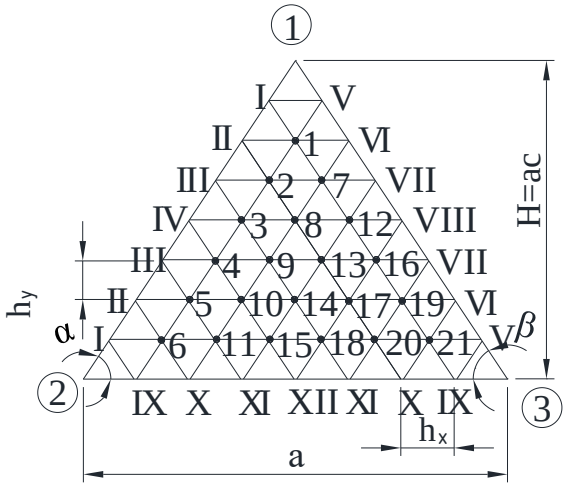

Figure 7 – Numbering of calculation nodes of the triangular grid

As a result of writing the finite difference equations (Table 1) for the calculated grid nodes (Figure 7), there is obtained a system of linear algebraic equations (SLAE)that has the following matrix form:

$$D \cdot \vec{F} = \vec{P}, \tag{12}$$

where $\vec{F}$ is the vector of nodal values of stress functions; $\vec{P}$ is the vector of the right part taking into account the load on the edges of triangular plates (formed in accordance with expressions (11); D is the square matrix of the 21st order (Figure 7) that is formed from the values of the grid parameters in accordance with expressions (5).

The SLAE (12) solution gives the values of the vector $\vec{F}$:

$$\vec{F} = D^{-1} \cdot \vec{P}, \tag{13}$$

where D^{-1} is the inverse matrix.

Then, based on the values of vector $\vec{F}$ (equation (13) there are calculated stresses at the nodes of the triangular grid according to formulas (3):

1) for the grid nodes inside the plate contour (taking into account Figure 2):

$$\sigma_{xi} = \frac{1}{h_y^2}[2(AB-1)F_i - AB(F_o + F_r) + A(F_p + F_s) + B(F_q + F_t)];$$

$$\sigma_{yi} = \frac{C^2}{h_y^2}(F_o - 2F_i + F_r); \tag{14}$$

$$\tau_{xy,i} = \frac{C^2}{h_y^2}(2(A-B)F_i - (A-B)(F_o + F_r) + (F_q + F_t) - (F_p + F_s).$$

2) for the grid nodes at the edges of the plate

a) on left edge (1-2) (Figures 3, a and 4):

$$\sigma_{n_1} = \frac{\partial^2 F}{\partial U^2} = \frac{\sin^2\alpha}{h_y^2}(F_q - 2F_i + F_t);$$

$$\sigma_u = \frac{\partial^2 F}{\partial n_1^2} = \frac{1}{h_y^2}\left\{\begin{array}{l} -2\left(A + U + AU\dfrac{\sin^2\alpha}{C^2}\right)F_i - \\ -AU\dfrac{\sin^2\alpha}{C^2}(F_q + F_t) + 2\left[(UF_r + AF_S) + h_y N_i\right] \end{array}\right\}, \tag{15}$$

$$\tau_{n_1,U} = \frac{\partial^2 F}{\partial n, \partial u} = \frac{2C}{h_y^2}(N_q - 2N_i + N_t).$$

b) on right edge (1-3) (Figures 3, b and 4):

$$\sigma_{n_2} = \frac{\sin^2\beta}{h_y^2}(F_p - 2F_i + F_s);$$

$$\sigma_\vartheta = \frac{1}{h_y^2}\left\{\begin{array}{l} -2\left(B + U + BU\dfrac{\sin^2\beta}{C^2}\right)F_i - \\ -BU\dfrac{\sin^2\alpha}{C^2}(F_p + F_s + 2\left[(UF_o + BF_t) + h_y N_i\right] \end{array}\right\}, \tag{16}$$

$$\tau_{n_1 r,\vartheta} = \frac{\partial^2 F}{\partial n_2 \partial \vartheta} = \frac{2C}{h_y^2}(N_p - 2N_i + N_s).$$

c) on edge (2-3) along the triangle base (Figure 3, c and 4):

$$\sigma_{xi}=\frac{1}{h_y^{\,2}}\left\{2(AB-1)F_i-AB(F_o+F_r)+2\left[\left(AF_p+BF_q\right)+h_y\cdot N_i\right]\right\};$$
$$\sigma_{yi}=\frac{C^2}{h_y^{\,2}}(F_o-2F_i+F_r);\ \ \tau_{xy,i}=\frac{\partial^2 F}{\partial x\partial y}=\frac{2C}{h_y^{\,2}}(N_o-2N_i+N_r). \quad (17)$$

On the oblique edges of the triangular plate (1-2), (1-3) (Figure 4), the stress along their normal and tangential directions (n_i (i=1, 2, u, υ)) is converted into stress along their Cartesian axes (x, y) using the following formulas:

a) at the nodes of left edge 1-2 (taking into account expressions (15)):

$$\sigma_x=\frac{0.5(\sigma_u-\sigma_{n_1})\cos(2\alpha)+0.5(\sigma_u+\sigma_{n_1})\cos(4\alpha)-\tau_{n_1,u}\sin(2\alpha)}{\cos(4\alpha)};$$
$$\sigma_y=\frac{0.5(\sigma_u-\sigma_{n_1})\cos(2\alpha)+0.5(\sigma_u+\sigma_{n_1})\cos(4\alpha)-\tau_{n_1,u}\sin(2\alpha)}{\cos(4\alpha)}; \quad (18)$$
$$\tau_{xy}=-\frac{0.5\left[\tau_{n_1u}\left(2\sin^2\alpha-1\right)+\sigma_u\sin(2\alpha)-\sigma_{n_1}\sin(2\alpha)\right]}{2\sin^2(2\alpha)-1};$$

b) at the nodes of right edge 1-3 (taking into account expressions (16)):

$$\sigma_x=\frac{0.5(\sigma_\vartheta-\sigma_{n_2})\cos(2\beta)+0.5(\sigma_\vartheta+\sigma_{n_2})\cos(4\beta)-\tau_{n_2,\vartheta}\sin(2\beta)}{\cos(4\beta)};$$
$$\sigma_y=\frac{0.5(\sigma_\vartheta-\sigma_{n_2})\cos(2\beta)+0.5(\sigma_\vartheta+\sigma_{n_2})\cos(4\beta)-\tau_{n_2,\vartheta}\sin(2\beta)}{\cos(4\beta)}; \quad (19)$$
$$\tau_{xy}=-\frac{0.5\left[2\tau_{n_2\vartheta}\left(2\sin^2\beta-1\right)+\sigma_\vartheta\sin(2\beta)+\tau_{n_2u}\sin(2\beta)\right]}{2\sin^2(2\beta)-1}.$$

To illustrate the theory of calculating the plane stress state of triangular plates based on the finite difference method (FDM) proposed here, we will consider the results of calculating an equilateral ($\alpha=\beta=60^0$) orthotropic triangular plate under uniform compression along the perimeter with a load of intensity "q" (Figure 7). Tables 2 and 3 show the results of calculating the plane stress state of an equilateral ($\alpha=\beta=60^0$) orthotropic triangular (for the conventional material) plate with the material orthotropy coefficients α_0=1734; β_0=2.0; (according to expressions (2)); q=1000 N/m.

Table 2 – Stresses in intra-contour nodes of orthotropic triangular plates

Grid node number (Figure 5)	Stresses, Pa ($\alpha=\beta=60^0$)					Stresses, Pa ($\alpha=45^0$; $\beta=60^0$)		
	$10^{-3}\sigma_{xi}$	$10^{-3}\sigma_{yi}$	$10^{-3}\tau_{xyi}$	Principal stresses		$10^{-3}\sigma_{xi}$	$10^{-3}\sigma_{yi}$	$10^{-3}\tau_{xyi}$
				$10^{-3}\sigma_1$	$10^{-3}\sigma_2$			
1	-1.034	-0.7161	0.00486	-0.0103	-1.7398	-0.7569	-0.2133	-0.416
2	-1.061	0.774	0.00634	-0.0523	-1.782	-0.60504	-0.54469	-0.1958
3	-1.04	-0.8423	0.0313	-0.0768	-1.806	-0.70168	-0.87142	-0.1929
4	0.975	-0.9374	-0.024	-0.0915	-1.821	-0.7299	-0.9884	-0.1432
5	-0.8287	-1.0159	-0.1483	-0.0575	-1.787	-0.74	-1.0347	-0.1147
6	-0.6256	-1.1154	-0.1943	-0.0087	-1.7353	-0.85567	-1.138	-0.1147
7	-1.049	-0.7488	-0.0046	-0.034	-1.7637	-0.8682	-0.4508	0.1238
8	-1.036	-0.6971	-0.0074	0.00188	-1.7314	-0.7111	-0.6438	-0.00205
9	-0.906	-0.7122	-0.175	-0.0555	-1.674	-0.711	-0.8243	-0.1489
10	-0.6894	-0.7705	-0.102	-0.1349	-1.594	-0.698	-0.9081	-0.19201
11	-0.3262	-0.7871	-0.2035	-9.3081	-1.421	-0.576	-0.8733	-0.19902
12	-1.041	-0.836	-0.026	-0.0748	-1.8037	-0.499	-0.5159	0.10643
13	-0.907	-0.7106	-0.1593	-0.0559	-1.6736	-0.7356	-0.6461	-0.00202
14	-0.6354	-0.7549	-0.0042	-0.1696	-1.556	-0.725	-0.8547	-0.00902
15	-0.3092	-0.8879	-0.0788	-0.266	-1.4631	-0.692	-0.9677	-0.1056
16	-0.9756	-0.9364	-0.022	-0.0913	-1.821	-0.8026	-0.8413	0.21903
17	-0.6899	-0.7698	-0.1018	0.1849	-1.5946	-0.776	-0.7669	-0.12471

18	-0.3094	-0.8874	-0.0707	0.2664	-1.4631	-0.7607	-0.9421	0.00356
19	-0.8288	-2.0159	0.0152	-0.0576	-1.7871	-0.8247	-1.0015	0.18969
20	-0.3264	-0.787	0.2035	0.30805	-1.4215	-0.7079	-0.8608	0.17969
21	-0.6256	-1.1154	0.1944	-0.0576	-1.7352	-0.8179	-1.0628	0.2117

Note: α_0=1,734; β_0=2,0; (q=1000 Н/м) = const

Table 3 – Stresses on the edges (contour nodes) of an equilateral orthotropic triangular plate

Stresses (10^{-3} σ_{ni}; 10^{-3} τ_{niui}) at the grid nodes (Figure 5)												
	On the left edge				**On the right edge**				**On the triangle base**			
	I	**II**	**III**	**IV**	**V**	**VI**	**VII**	**VIII**	**IX**	**X**	**XI**	**XII**
σ_{n1}	-1.0	-1.0	-1.0	-1.0	-	-	-	-	-	-	-	-
σ_u	-5.8556	-9.5018	-11.727	-12.549	-	-	-	-	-	-	-	-
τ_{n1u}			0.0		-	-	-	-	-	-	-	-
σ_{n2}	-	-	-	-	-1.0	-1.0	-1.0	-1.0	-	-	-	-
σ_υ	-	-	-	-	-5.947	-9.729	-11.918	-12.554	-	-	-	-
$\tau_{n2\upsilon}$	-	-	-	-			0.0					
$\sigma_{n3}(\sigma_y)$	-	-	-	-	-	-	-	-	-1.0	-1.0	-1.0	-1.0
σ_x	-	-	-	-	-	-	-	-	-1.28	-1.994	-2.578	-2.728
τ_{n3x}	-	-	-	-	-	-	-	-			0.0	

Figures 8 and 9 show the stress diagrams σ_{xi} (along section I-1-7-14-XII) and σ_{yi} (along section 2-IX-X-XI-XII; taking into account symmetry).

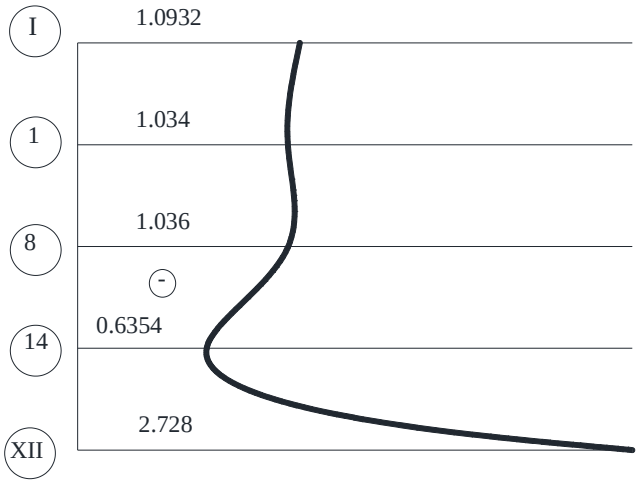

Figure 8 – Stress curve (σ_{xi} 10^{-3}), Pa [over section (I-1-8-14-XII)]

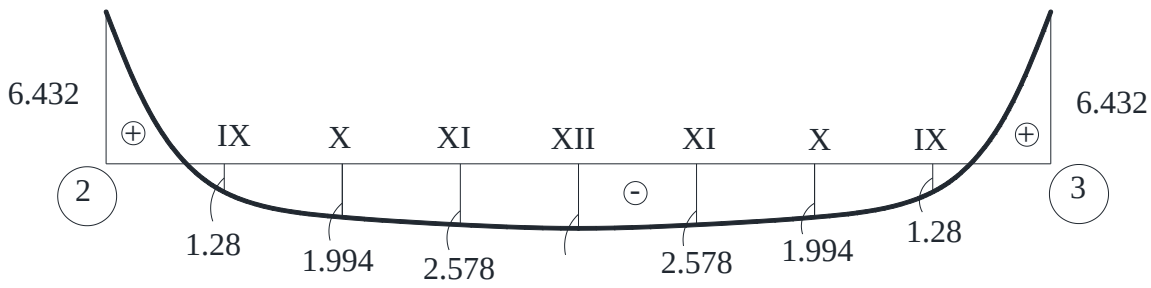

Figure 9 – Stress curve (σy_i 10^{-3}, Pa) (over section (2-IX-X-XI-XII))

Tables 4 and 5 show the stress values at the grid nodes (Figure 7) depending on changing the angles α and β, as well as changing the orthotropy coefficients α_0, β_0; Figures 10 and 11 show graphic images depending on these values.

Table 4 – Stress dependence on the angles α and β

Values of the α angle	Other constant parameters	Current stresses, Pa									Principal stresses, Pa					
		$(\sigma x_i)\cdot 10^{-3}$			$(\sigma y_i)\cdot 10^{-3}$			$(\tau xy,i)\cdot 10^{-3}$			$(\sigma_{1,i})\cdot 10^{-3}$			$(\sigma_{2,i})\cdot 10^{-3}$		
		***i*=8**	**10**	**17**	**8**	**10**	**17**	**8**	**10**	**17**	**8**	**10**	**17**	**8**	**10**	**17**
15^0	$\beta=60^0$=const; α_0=1,.34; β_0=2.0 (q = 1000 N/m) = const.	1.13	-0.85	-1.81	-0.72	-1.00	-0.89	-0.24	-0.10	0.12	4.22	5.09	2.67	-3.81	-4.97	-5.35
30^0		-0.21	-0.75	-1.04	-0.68	-0.99	-0.84	-0.14	-0.18	0.08	0.97	0.54	0.48	-1.86	-2.29	-2.36
45^0		-0.71	-0.7	-0.78	-0.64	-0.91	-0.77	0	-0.19	0.17	0.18	0.06	0.09	-1.54	-1.66	-1.63
60^0		-1.03	-0.69	-0.69	-0.70	-0.77	-0.77	0	-0.10	0.10	0	0.14	0.14	-1.73	-1.59	-1.59
90^0		-2.13	-0.8	-1.02	-1.52	-0.84	-0.54	-0.26	0.29	-0.28	0.42	1.42	1.46	-4.07	-3.07	-3.02

Table 5 – Stress dependence on the orthotropy coefficients

Values of α_0	Other constant parameters	Current stresses, Pa									Principal stresses, Pa					
		$(\sigma x_i)\cdot 10^{-3}$			$(\sigma y_i)\cdot 10^{-3}$			$(\tau xy,i)\cdot 10^{-3}$			$(\sigma_{1,i})\cdot 10^{-3}$			$(\sigma_{2,i})\cdot 10^{-3}$		
		***i*=8**	**10**	**17**	**8**	**10**	**17**	**8**	**10**	**17**	**8**	**10**	**17**	**8**	**10**	**17**
0.5	(α=β=600)=const; β_0=2.0 (q = 1000 N/m) = const.	-1.13	-0.66	-0.66	-0.20	-0.80	-0.79	0	-0.09	0.09	0.05	0.19	0.14	-1.88	-1.64	-1.64
1.0		-1.09	-0.67	-0.67	-0.76	-0.79	-0.79		-0.09	0.09	-0.04	0.15	0.15	-1.80	-1.61	-1.61
1.5		-0.05	-0.68	-0.68	-0.76	-0.78	-0.77	0	-0.10	0.10	0	0.14	0.14	-1.75	-1.60	-1.60
1.73		-1.04	-0.69	-0.69	-0.70	-0.77	-0.77	0	-0.10	0.10	0	0.13	0.13	-1.73	-1.59	-1.59
2.0		-1.02	-0.69	-0.69	-0.68	-0.77	-0.76	0	-0.10	0.10	0.02	0.14	0.14	-1.71	-1.59	-1.59
2.5		-1.99	-0.70	-0.70	-0.64	-0.76	-0.75	0	-0.11	0.11	0.06	0.14	0.14	-1.68	-1.60	-1.60

Figures 10 and 11 show the graphical dependencies of the stresses at the design point i=8 (Figure 7) with a change in the value of the angles α and β, as well as with a variation in the orthotropy parameters α_0, β_0.

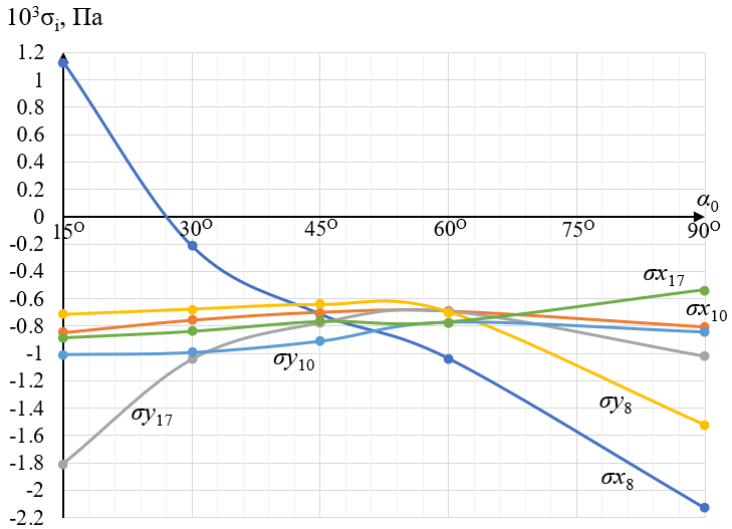

Figure 10 – Stresses (σx_i, σy_i) dependence on the α angle ($\beta=60^0$=const)

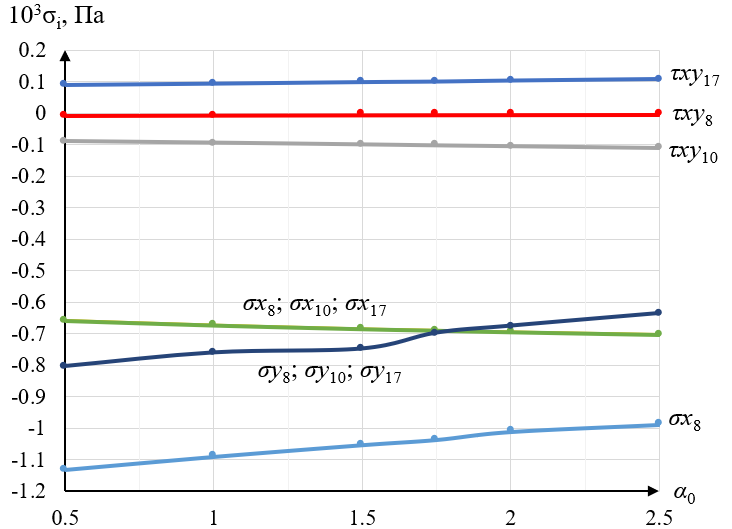

Figure 11 – Stresses (σx_i, σy_i) dependence on the orthotropy coefficients of α_0 (β_0=2.0=const)

To assess reliability of the results obtained by the authors that confirm the above theoretical positions, an alternative calculation of an equilateral orthotropic triangular plate was performed with the same initial data; the obtained pattern and values of stresses of the plane stress state are quite close (Figure 12, Table 6 in [21]) to those given in Tables 2 and 3.

In the course of the study, a comparative evaluation of the stress-strain state (SS) of a triangular plate under plane stress state was carried out using two numerical methods: the finite difference method (FDM) and the finite element method (FEM) implemented in the ANSYS software environment. Comparison of stress distribution in the fields of normal stresses σ_x, σ_y, and tangential stresses τ_{xy} obtained by both methods shows a qualitatively similar distribution pattern (Figure 12). The highest stresses are observed in the areas of load concentration and geometric features, which is consistent with the expected physical patterns. The stress values obtained at the nodal points show good quantitative agreement. The maximum relative error between the results does not exceed 2%, indicating good convergence of the solutions despite different numerical approaches.

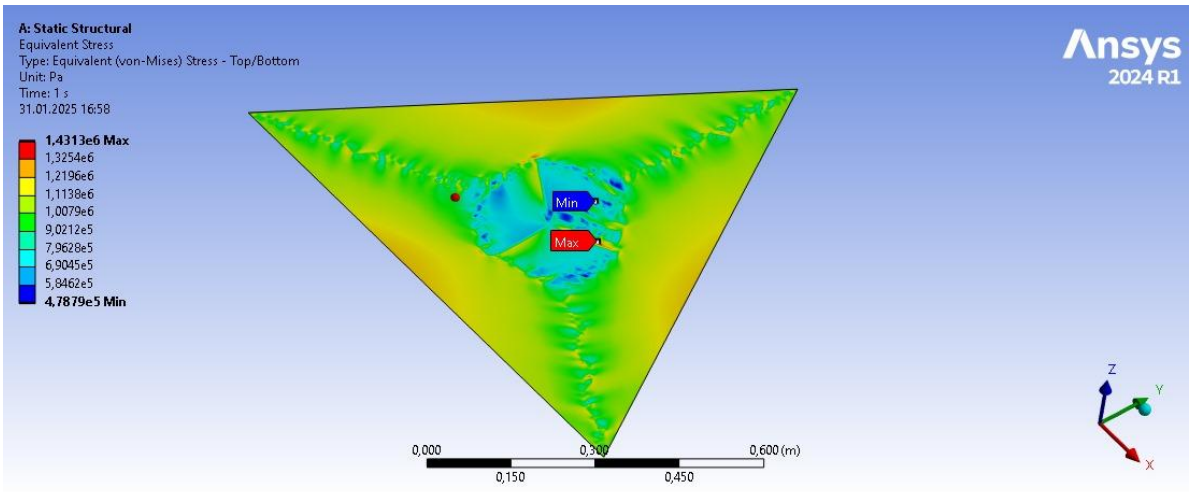

Figure 12 – Equivalent stresses

The finite difference method proved to be quite accurate for relatively simple triangular geometry and regular mesh, but its application becomes difficult for complex boundary conditions. In contrast, the finite element method in ANSYS is more flexible in constructing the computational model, especially in the presence of arbitrary geometry and inhomogeneous loading conditions.

Nevertheless, with adequate discretization and consideration of boundary conditions, the FEM is capable of producing results close to those obtained in ANSYS. This emphasizes the practical applicability of ICR in engineering analysis problems, especially in conditions of limited computational resources.

4. Conclusions

1. In this study, the plane stress state of orthotropic triangular plates was analyzed using the numerical finite difference method (FDM) based on a grid of scalene triangles. The results obtained allow drawing a number of important conclusions that can be useful both for further scientific research and for practical application in the design of thin-walled structures.
2. Using the well-known FDM procedure, resolving finite difference equations were obtained that took into account the plate geometry (angles α and β), orthotropic properties of materials (coefficients α_0 and β_0), loading in the midplane in the form of a plate distributed over part of the edges (parameters u_0, υ_0 (Figure 1)).
3. The recording of boundary conditions is shown based on the analogy for a grid of scalene triangles in accordance with the idea of pairwise exclusion of stress functions in the contour and edge nodes of the grid (expressions 8-10); here there are also given typical finite-difference equations near

the edges and at the apexes of a triangular plate (Table 1) which allows solving problems of the plane stress state for arbitrary values of the "oblique" angles (α and β) of the lateral edges of the plate.

4. Finite-difference equations of stresses (σx, σy, τxy) in the median plane for a grid of scalene triangles (including the nodes located on the edges of the plates) were obtained.

5. The authors of the article developed a special program for calculating the plane stress state (with the grid density of N=8) with a height of degree of automation for calculating all the types of stress in the median plane.

6. Using this program, a number of research problems were solved with variable parameters α and β; α_0 and β_0; u_0 and υ_0; they are presented in tabular and graphical forms.

7. The following was established:

a) for orthotropic equilateral triangular plates ($\alpha=\beta=60^0$), the stresses at the grid nodes will be symmetrical only in the direction of one median (to the base of the triangle); while for isotropic triangular plates, there are three axes of elastic symmetry (along all three medians);

b) for the diagrams in Figures 8, 9 the known conditions of equilibrium of external and internal forces are fulfilled, when the area of the diagrams (σx and σy) in different directions is equal to the resultant of external forces in the same directions, which indirectly confirms the reliability of the theoretical positions and results presented by the authors;

c) for orthotropic triangular plates, even under uniform compression along the perimeter, there is a non-uniform stress state (compared to similar isotropic triangular plates);

d) the following patterns can be traced in Figures 10, 11: the highest stress (σx_{17}) occurs at $\alpha=45^0$; $\beta=60^0$ (Figure 10); at ($\alpha=\beta=60^0$) all the stress values (σx_8, σx_{10}, σx_{17}, σy_8, σy_{10}, σy_{17}) are close to each other as established based on the graphs and tables provided. The effect of the orthotropy coefficients on the stress values σxi, σyi turned out to be insignificant.

8. To verify the reliability of the obtained results, an alternative calculation was performed in the ANSYS program. The results obtained using the FDM turned out to be quite close to the data obtained in ANSYS, which confirmed the correctness of the proposed method and its applicability for solving problems of the plane stress state of orthotropic triangular plates.

9. The presented theoretical provisions and numerical results of the plane stress state of orthotropic triangular plates can serve as a basis for subsequent research into the stability problems of orthotropic triangular plates under non-uniform stress conditions.

10. The algorithm for calculating the plane stress state of orthotropic triangular plates proposed by the authors of this work can be widely used both in research problems of solid mechanics and in the practical design of thin-walled structures used as load-bearing elements of various buildings, engineering structures, mechanisms, and machines.

References

[1] S. K. Akhmediyev, *Calculation of triangular plates*. Karaganda: KSTU, 2006.

[2] M. Eröz, "Stress analysis of a pre-stretched orthotropic plate with finite dimensions," *Transactions of the Canadian Society for Mechanical Engineering*, vol. 45, no. 2, pp. 346–354, Jun. 2021, doi: 10.1139/tcsme-2019-0241.

[3] Y. Xu and Z. Wu, "Exact solutions for rectangular anisotropic plates with four clamped edges," *Mechanics of Advanced Materials and Structures*, vol. 29, no. 12, pp. 1756–1768, May 2022, doi: 10.1080/15376494.2020.1838007.

[4] Q. Yu, "A hierarchical wavelet method for nonlinear bending of materially and geometrically anisotropic thin plate," *Commun Nonlinear Sci Numer Simul*, vol. 92, p. 105498, Jan. 2021, doi: 10.1016/j.cnsns.2020.105498.

[5] J. Petrolito and D. Ionescu, "Alternative Low-Order Triangular Elements for Thick and Thin Shell Analysis," *Int J Comput Methods*, vol. 22, no. 03, Apr. 2025, doi: 10.1142/S0219876223420069.

[6] Z. Celep, Z. Özcan, and A. Güner, "Elastic triangular plate dynamics on unilateral Winkler foundation: Analysis using Chebyshev polynomial expansion for forced vibrations," *Journal of Mechanical Science and Technology*, vol. 39, no. 1, pp. 65–79, Jan. 2025, doi: 10.1007/s12206-024-1207-5.

[7] T. Führer and N. Heuer, "Mixed finite elements for Kirchhoff–Love plate bending," *Math Comput*, Jul. 2024, doi: 10.1090/mcom/3995.

[8] Q. Liang, "Corotational Hinge-based Thin Plates/Shells," *Computer Graphics Forum*, Apr. 2025, doi: 10.1111/cgf.70022.

[9] M. Epstein and P. Vernon, "A triangular fractal plate bending element," *Zeitschrift für angewandte Mathematik und Physik*, vol. 75, no. 5, p. 163, Oct. 2024, doi: 10.1007/s00033-024-02300-0.

[10] A. M. Katili, K.-U. Bletzinger, and I. Katili, "An optimum triangular plate element based on DSPM with incomplete quadratic functions and an assumed orthogonality condition," *Comput Struct*, vol. 296, p. 107301, Jun. 2024, doi: 10.1016/j.compstruc.2024.107301.
[11] S. K. Akhmediyev, M. Y. Zhakibekov, I. A. Kurokhtina, and Z. S. Nuguzhinov, "Numerical study of stressed and strained state of thin walled structure of triangular plate type of small and middle thickness," *Structural Mechanics and Analysis of Constructions*, no. 2, pp. 28–33, 2015.
[12] A. V. KOROBKO, N. G. KALASHNIKOVA, and E. G. ABASHIN, "Transverse bending and free vibrations of elastic isotropic plates in the form of isosceles triangles," *Building and reconstruction*, vol. 98, no. 6, pp. 20–27, 2021, doi: 10.33979/2073-7416-2021-98-6-20-27.
[13] V. Korobko and S. Savin, "Free vibration of the triangular orthotropic plate with homogeneous and combined boundary conditions ," *Building and reconstruction*, vol. 46, no. 2, pp. 33–40, 2013.
[14] M. S. Beketova *et al.*, "Bending of orthotropic scalene triangle plates: finite difference modeling," *Magazine of Civil Engineering*, vol. 17, no. 7, p. 13407, 2025, doi: 10.34910/MCE.134.7.
[15] O. Ya. Grigorenko, M. Yu. Borisenko, O. V. Boichuk, and L. Ya. Vasil'eva, "Free Vibrations of Triangular Plates with a Hole*," *International Applied Mechanics*, vol. 57, no. 5, pp. 534–542, Sep. 2021, doi: 10.1007/s10778-021-01104-3.
[16] D. Cai, X. Wang, and G. Zhou, "Static and free vibration analysis of thin arbitrary-shaped triangular plates under various boundary and internal supports," *Thin-Walled Structures*, vol. 162, p. 107592, May 2021, doi: 10.1016/j.tws.2021.107592.
[17] M. Sathyamoorthy, "Effects of large amplitude and transverse shear on vibrations of triangular plates," *J Sound Vib*, vol. 100, no. 3, pp. 383–391, Jun. 1985, doi: 10.1016/0022-460X(85)90294-9.
[18] D. He, T. Liu, B. Qin, Q. Wang, Z. Zhai, and D. Shi, "In-plane modal studies of arbitrary laminated triangular plates with elastic boundary constraints by the Chebyshev-Ritz approach," *Compos Struct*, vol. 271, p. 114138, Sep. 2021, doi: 10.1016/j.compstruct.2021.114138.
[19] S. K. Akhmediyev, O. Khabidolda, N. I. Vatin, G. A. Yessenbayeva, and R. Muratkhan, "Physical and mechanical state of cantilever triangular plates," *Journal of Mathematics, Mechanics and Computer Science*, vol. 118, no. 2, pp. 64–73, Jul. 2023, doi: 10.26577/JMMCS.2023.v118.i2.07.
[20] Y. Yang, D. An, H. Xu, P. Li, B. Wang, and R. Li, "On the symplectic superposition method for analytic free vibration solutions of right triangular plates," *Archive of Applied Mechanics*, vol. 91, no. 1, pp. 187–203, Jan. 2021, doi: 10.1007/s00419-020-01763-7.
[21] Varvak. P.M. and Varvak. L.P., *Method of grids in calculations of building structures*. Moscow: Stroyizdat, 1977.

Information about authors:

Moldir Beketova – PhD Student, A.S. Saginov Karaganda Technical University, Karaganda, Kazakhstan, moldir-9292@mail.ru
Zhmagul Nuguzhinov – Dr. Eng., Professor, Director of the Kazakhstan Multidisciplinary Institute of Reconstruction and Development (KazMIRR), Karaganda, Kazakhstan, kazmirr@mail.ru
Serik Akhmediyev – Candidate of Technical Sciences, Professor, A.S. Saginov Karaganda Technical University, Karaganda, Kazakhstan, serik.akhmediyev@mail.ru
Valentin Mikhailov – Candidate of Technical Sciences, Associate Professor, A.S. Saginov Karaganda Technical University, Karaganda, Kazakhstan, v.mihaylov@kstu.kz
Omirkhan Khabidolda – PhD, E.A. Buketov Karaganda University, Karaganda, Kazakhstan, oka-kargtu@mail.ru

Author Contributions:

Moldir Beketova – data collection, visualization, drafting.
Zhmagul Nuguzhinov – editing, testing, modeling, drafting.
Serik Akhmediyev – methodology, resources, analysis.
Valentin Mikhailov – analysis, interpretation, modeling.
Omirkhan Khabidolda – interpretation, modeling, methodology

Conflict of Interest: The authors declare no conflict of interest.

Use of Artificial Intelligence (AI): The authors declare that AI was not used.

Received: 03.03.2025
Revised: 10.06.2025
Accepted: 12.06.2025
Published: 13.06.2025